Divergent Barotropic Instability of the Tropical Asymmetric Easterly Jet

S. K. MISHRA, D. SUBRAHMANYAM AND M. K. TANDON

Indian Institute of Tropical Meteorology, Pune-411 005

(Manuscript received 29 October 1980, in final form 11 May 1981)

ABSTRACT

The divergent barotropic instability of a zonally averaged, observed, tropical, upper tropospheric, monsoon easterly jet is investigated by numerical integration of a linear spectral model. The Rossby radius of deformation for the upper troposphere is computed from a three-layer model of the atmosphere. It is shown that the antisymmetric zonal flow components in the jet contribute in stabilizing the short waves and destabilizing the long waves. Furthermore, the maximum amplitude of the asymmetric preferred wave is shifted southward (to 6°N) to a region where a largest positive maximum of $-\bar{u}_{yy}$ is located for the asymmetric profile. A large decrease in the meridional scale of the wave and a threefold increase in the ratio of the computed maximum southward-to-northward easterly momentum transports is also found for the asymmetric jet compared to the symmetric jet. The divergence is found to increase the growth rates of all the waves and, also to increase the preferred wavelength.

The most unstable divergent asymmetric wave is shown to have a wavelength of 6500 km, an e-folding time of 6.5 days and a westward phase speed of 23.5 m s^{-1}. The zonal scale of the preferred wave is nearly equal to the Rossby radius of deformation.

1. Introduction

The observational studies of upper tropospheric tropical circulation during the northern summer by Koteswaram (1958), Krishnamurti (1971) and others have shown that the monsoonal easterly jet is a set of westward propagating synoptic-scale transient waves. The spectral analysis of barotropic energy exchange for the summer season of 1967 by Kanamitsu *et al.* (1972) has indicated that these waves have a horizontal scale of the order of 5000–7000 km. The *in situ* formation due to barotropic instability of the jet is widely assumed as one of the possible sources of energy for these waves, as indicated by the observed equatorward transport of easterly momentum due to transient eddies at the jet level. However, a recent study by Mishra and Salvekar (1980) has shown that the jet also is baroclinically unstable with a preferred wavelength comparable to the observed upper tropospheric waves. In order to understand the observed meridional scale of the waves and the westerly momentum transport associated with them, a barotropic instability analysis is performed in this study.

The momentum transport, which is everywhere equatorward (Newell *et al.*, 1972) with higher values in the southern than in the northern region of the jet core, indicates not only a possible transfer of kinetic energy from basic flow to the disturbances, but also the possible important role for the jet's meridional asymmetry (Lipps, 1966). Yamasaki and Wada (1972) have studied the instability of an idealized symmetric easterly jet by neglecting the observed zonal and meridional asymmetries. Tupaz *et al.* (1978) considered the zonal asymmetry alone in the jet and obtained different local growth rates for the disturbances located in different zonal regions. Shukla (1977) has studied the barotropic instability of the mean July profile of zonal wind at the 150 mb level along 85°E and obtained a preferred wavelength of 3000 km, which is less than the observed wavelengths of the upper tropospheric disturbances as mentioned above. All of these studies are based on a nondivergent barotropic model.

The study of Colton (1973) clearly shows that the instability of the jet is not uniform in the zonal direction. Colton examined the mean 200 mb flow of June–August 1967 and pointed out that the large localized meridional vorticity gradients satisfy the nondivergent barotropic instability criterion. However, the divergent barotropic instability criterion is less stringent for an easterly jet compared to that of a westerly jet as shown by Lipps (1963). Philander (1976) has shown that divergence destabilizes the barotropic waves in tropical easterlies. Thus, it is expected that a significant contribution to the instability of the jet may arise due to divergence effect.

A spectral technique based on a truncated Fourier series approximation is used to obtain the numerical solution in this study, because it is simpler by this method to include or exclude the meridionally antisymmetric zonal flow components. Wiin-Nielsen

0022-4928/81/102164-08$06.00
© 1981 American Meteorological Society

(1961) and Haltiner and Song (1962) have used the same method to study the stability characteristics of jet profiles. Furthermore, Haltiner and Song also compared the solutions obtained by this method with those from a finite-difference method for single and double jet profiles and found reasonable agreement in the solutions. Simmons (1974) has discussed the applicability of this method and computed the accuracy of the solutions obtained for a midlatitude flow, and thereby concluded that the method is accurate enough for the instability studies.

Thus, we propose to examine the divergent barotropic instability of the observed mean easterly jet and the role of its antisymmetric components, by utilizing the truncated Fourier series method.

2. System of equations

a. Model equations and boundary conditions

It is well known that the upper tropospheric wave disturbances seldom propagate downward to the lower troposphere. This also can be concluded from the observed momentum transports which are essentially confined in the 400–100 mb layer. Based on this fact, a three-layer system is formulated. The motionless top and the bottom layers correspond to the lower stratosphere and the lower troposphere, respectively, and the active middle layer represents the upper troposphere (the region of observed easterly jet) which is in motion. Furthermore, the flow in the middle layer is assumed to be in quasi-geostrophic equilibrium, because the required conditions in terms of Rossby and Richardson numbers are approximately satisfied. The meridional scale of the observed basic zonal flow is comparable to the Rossby radius of deformation, justifying the inclusion of divergence effect in the model.

The equations for the simplified, divergent, quasi-geostrophic three-layer model appropriate to the present problem are obtained by considering each of the three layers as a homogeneous, incompressible, non-viscous non-mixing barotropic fluid, with the top, middle and bottom layers having potential temperatures θ_t, θ_m and θ_b, respectively. The three-layer system is assumed to be gravitationally stable ($\theta_b < \theta_m < \theta_t$) and the top and bottom layers are infinitely deep. The middle layer has a constant depth H when at rest. The linearized potential vorticity equation for the perturbations in the middle layer on a beta plane may be written as

$$\frac{\partial}{\partial t}(\nabla^2\psi - \mathrm{Ro}^{-2}\psi) + \bar{u}\frac{\partial}{\partial x}(\nabla^2\psi - \mathrm{Ro}^{-2}\psi) + (\beta - \bar{u}_{yy} + \mathrm{Ro}^{-2}\bar{u})\frac{\partial\psi}{\partial x} = 0, \quad (1)$$

where $\psi = ghf_0^{-1}$ is the perturbation streamfunction, h the perturbation depth of the middle layer, $\bar{u}(y)$ the basic-state geostrophic zonal wind, f_0 the Coriolis parameter, g the acceleration due to the earth's gravity and Ro, the Rossby radius of deformation, which is given by

$$\mathrm{Ro} = (g^*H)^{1/2}f_0^{-1}. \quad (2)$$

Finally, g^* is the reduced gravity given as

$$g^* = g(\theta_t - \theta_m)(\theta_m - \theta_b)\theta_m^{-1}(\theta_t - \theta_b)^{-1}. \quad (3)$$

The three-layer system is confined between two rigid vertical walls at a distance D. The appropriate lateral boundary conditions for the model are that v-component of the perturbation wave motion vanishes at the walls or equivalently

$$\psi = 0 \quad \text{at} \quad y = 0 \text{ and } D. \quad (4)$$

b. Numerical technique

An initial value approach is used for computing the phase speeds and the growth rates of all unstable waves in the model. Integration of (1) was performed in a wavenumber domain with a truncated sine series representation for ψ field and a cosine series representation for $\bar{u}(y)$, in the y direction, since the sequence of sine functions in the interval $0 \leq y \leq D$ forms an orthogonal set and also satisfies the boundary conditions of the model. In order to close the spectral form of (1), in one-dimensional meridional wavenumber space, it is essential to present $\bar{u}(y)$ as a cosine series. We consider the perturbation as a wave of wavenumber k in the zonal direction. Then, $\bar{u}(y)$ and ψ can be represented as

$$\bar{u}(y) = \sum_{n=0}^{N} u_n \cos nly \quad (5)$$

and

$$\psi(x, y, t) = \sum_{m=1}^{M} [\psi_{1m}(t)\cos kx + \psi_{2m}(t)\sin kx]\sin mly, \quad (6)$$

where $l = \pi/D$ is the meridional wavenumber, u_n and (ψ_{1m}, ψ_{2m}) denote the expansion coefficients of $\bar{u}(y)$ and ψ, respectively, and N and M denote the order of meridional wavenumber truncations for $\bar{u}$ and ψ, respectively. Each term of (5) and (6) represents one spectral or meridional wave component.

The spectral version of the vorticity equation is obtained by substituting Eqs. (5) and (6) in (1). The resulting spectral equations (not given here) are coupled differential equations in $\psi_{11}, \ldots, \psi_{1M}; \psi_{21}, \ldots, \psi_{2M}$, which are numerically integrated by utilizing the modified Euler-backward time-differencing scheme for the first time step and the leapfrog scheme for subsequent time steps with a time step of 60 min. In order to dampen tem-

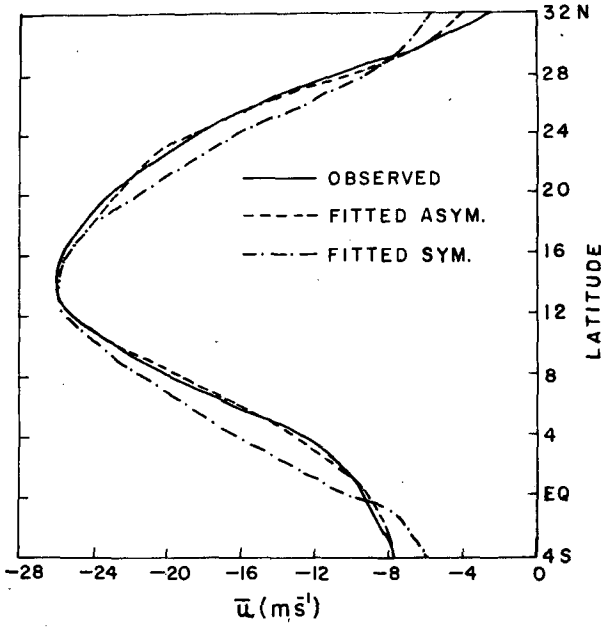

FIG. 1. Meridional profiles of the observed, and fitted asymmetric and symmetric, zonal wind at the 100 mb level for a truncation $N = 6$.

poral oscillations of the solutions, the time filter of Robert (1966) was used. The filter parameter was set equal to 0.01 as used by others. The exponential solutions of sufficient accuracy were obtained by ensuring that the relative error between two consecutive six hourly averaged growth rates were $<10^{-4}$. Initially $\psi_{2m} = 0$; ψ_{1m} had a Gaussian distribution in m with the center at $m = 0$ and the standard deviation of unity for $m = 1, \ldots, M$, were chosen.

c. Growth rate and phase speed

The meridional spectrum of phase speed (c_m) and the growth rate (ν_m) at each time step are computed from

$$c_m = k^{-1} \frac{d}{dt} \delta_m, \tag{7}$$

$$\nu_m = \frac{1}{2} \frac{d}{dt} (\ln \mathrm{KE}_m), \tag{8}$$

where $m = 1, 2, \ldots, M$, the phase angle δ_m denotes the location of the wave trough and is given by

$$\delta_m = \tan^{-1}(-\psi_{2m}/-\psi_{1m}).$$

and KE_m is the horizontally averaged kinetic energy per unit mass of the wave computed from

$$\mathrm{KE}_m = \tfrac{1}{8}(\psi_{1m}^2 + \psi_{2m}^2)(k^2 + m^2 l^2).$$

It is easily understood that all of the meridional modes of the exponential growing wave have same phase speed and growth rates. The attainment of the uniformity in the growth rate and the phase speed spectrum in course of the time integration of the model is indicative of the fact that the wave has reached a state of uniform exponential growth.

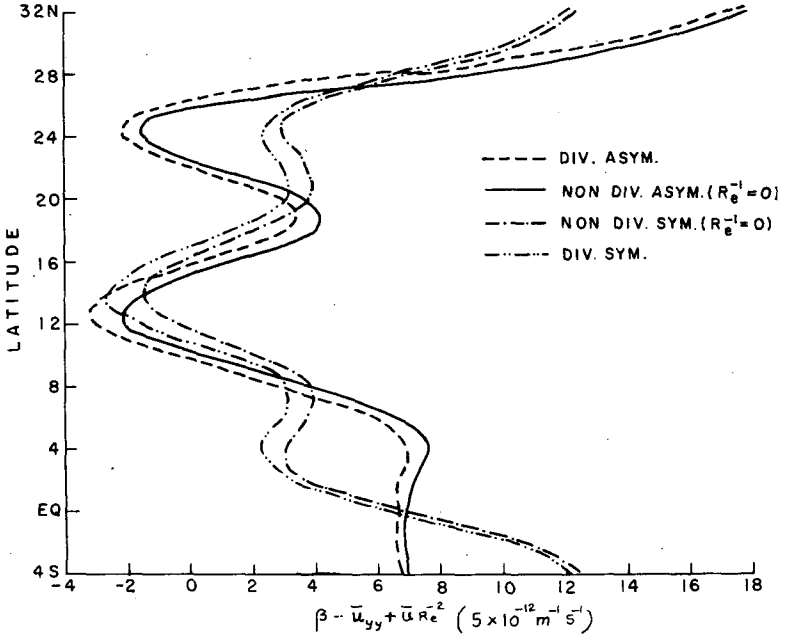

FIG. 2. Meridional profiles of $(\beta - \bar{u}_{yy} + \mathrm{Ro}^{-2}\bar{u})$ for the nondivergent asymmetric, divergent asymmetric, nondivergent symmetric and divergent symmetric cases.

This criterion is also utilized for the termination of the time integration of the model.

3. Model parameters

The physical parameters in the model have been chosen as $f_0 = 3.77 \times 10^{-5}$ s^{-1} and $\beta = 2.211 \times 10^{-11}$ m^{-1} s^{-1} the values corresponding to 15°N, the observed mean latitude of the easterly jet over the Indian region. For determining the reduced gravity g^*, we have considered the 1000–500, 500–100 and 100–10 mb layers of the atmosphere and their vertically averaged potential temperatures as the bottom, the middle and the top layers of the model and their potential temperatures, respectively. From the observed seasonal potential temperatures at standard isobaric levels in the belt (5°S–30°N), for summer, we have determined

$$\theta_b = 310.5 \text{ K}, \quad \theta_m = 343.0 \text{ K} \quad \text{and} \quad \theta_t = 521.1 \text{ K}.$$

The computed value of the reduced gravity is found to be 0.786 m s^{-2}, which is less than $\frac{1}{12}$ of g.

The depth of the middle layer H is computed by considering it as an isothermal layer with a temperature equal to the average temperature of the middle layer. H is assumed to be equal to the depth corresponding to the pressure fall of 400 mb with the constant average density of the layer. The value of H so determined is 9 km which is nearly equal to an average of the scale height and geometric depth of the upper troposphere. The Rossby radius of deformation is computed from (2) by using the above values of g^* and H, and found to be 2225 km. In order to check the validity of the above formulation, Ro also was computed by using its definition in terms of the buoyancy frequency and it was found that the two values are in good agreement.

4. Spectral representation of the basic flow

The monsoon seasonal (June–August) normal zonal winds at the 100 mb level, in the region 8°S–36°N and 70–120°E are picked up on a regular grid of 2°(Δy) latitude and 5° longitude. These values are subjected to a five point filter along the latitudes.

$$u_j^* = -\tfrac{1}{12}u_{j-2} + \tfrac{1}{4}u_{j-1} + \tfrac{2}{3}u_j + \tfrac{1}{4}u_{j+1} - \tfrac{1}{12}u_{j+2}, \quad (9)$$

where the asterisk denotes filtered values. The filter (9) eliminated the $2\Delta y$ wave completely and damped all the other waves up to $6\Delta y$, with 50% damping for the $3\Delta y$ wave. The waves longer than $6\Delta y$ show a small amplification of <2%. The filtered data is used for computing u_n. We have chosen a truncation $N = 6$ for $\bar{u}$, because the first seven coefficients are found to explain more than 99% of the observed variance, which can also be seen from the closeness of fit between the observed and fitted profiles as presented in Fig. 1. A symmetric profile of $\bar{u}$ is obtained by considering the even coefficients u_0, u_2, u_4, u_6 alone, which explained 92% of the fitted variance. Although the variance contribution by antisymmetric components (8%) is very small, they may still play a crucial role in the instability characteristics of the jet. This can particularly be seen from the ($\beta - \bar{u}_{yy}$) profiles for four different cases

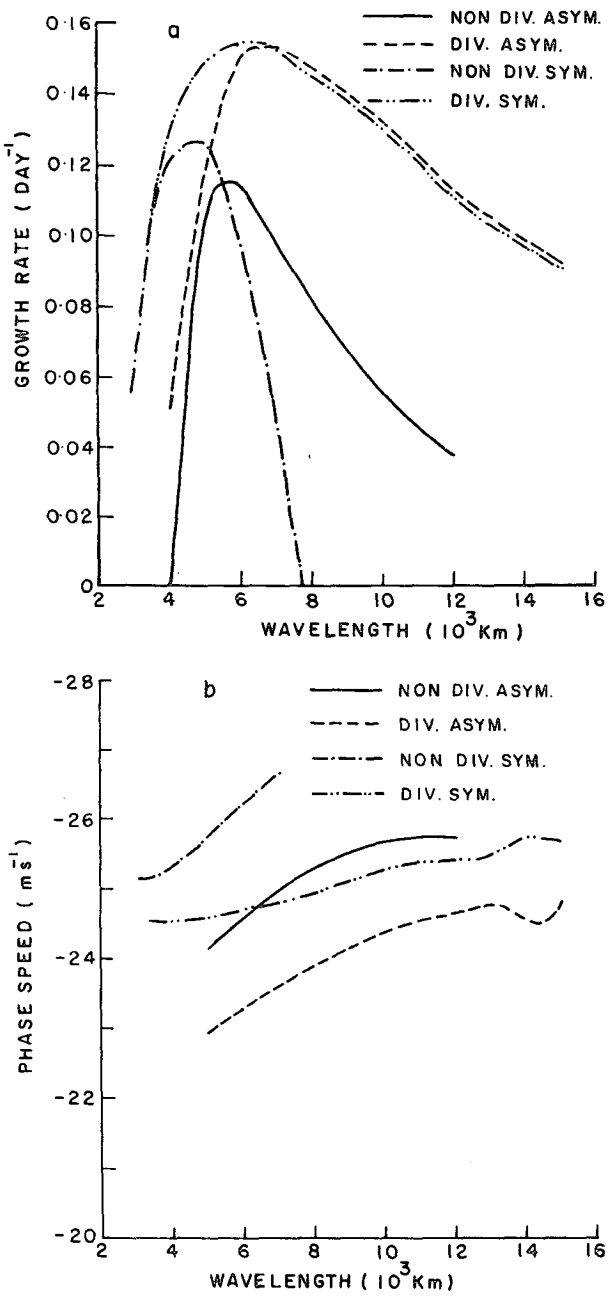

FIG. 3. (a) Growth rates and (b) phase speeds as functions of wavelength for the four cases.

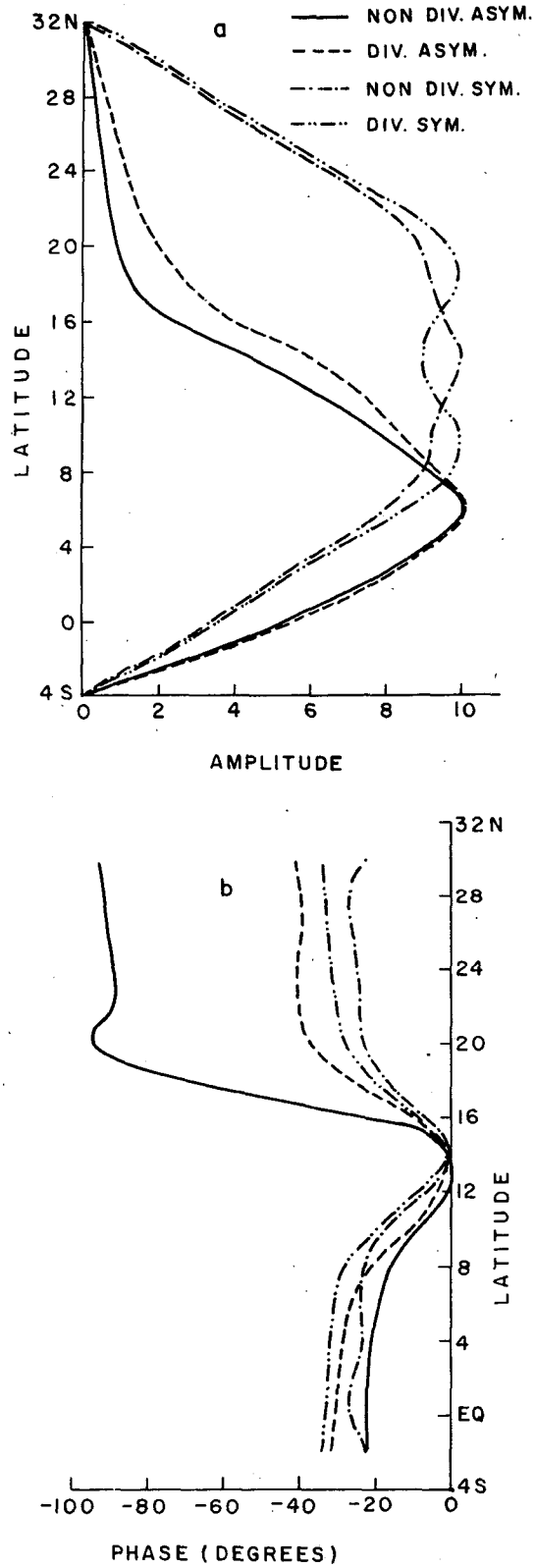

FIG. 4. (a) Normalized meridional amplitude and (b) phase profiles of the preferred waves for the four cases.

as shown in Fig. 2. In these profiles the antisymmetric components contained ~37.5% variance of the asymmetric profile. The meridional scale of the easterly jet, determined as the distance over which the wind speed is equal to or more than half of its maximum value, is found to be 2600 km. This scale is more than the Rossby radius of deformation. The radius of curvature of the jet at its center is computed to be 1000 km. These two scales will be used in connection with the discussion regarding meridional scale of unstable waves.

5. Results

The results were obtained with the different initial conditions. It was seen that the time required by the waves to reach an exponential state depends on the initial conditions, while the growth rate, phase speed and structure of the exponentially growing wave are independent of the initial conditions. It was noticed that the model is able to reproduce with a good accuracy the results as obtained in the other barotropic studies by utilizing an eigenvalue approach.

The numerical solutions obtained from the model correspond to the fastest growing mode. The growth rates and phase speeds of this mode of the wave for different zonal wavelengths in the range of 3000 to 15 000 km are computed for the following cases of the easterly jet: (i) nondivergent asymmetric, (ii) divergent asymmetric, (iii) nondivergent symmetric and (iv) divergent symmetric. A truncation $N = 6$ and $M = 12$ is used for obtaining the numerical solution. This truncation is found to be sufficient for this study. Some of the growth rate and phase speed curves in the Figs. 3a and 3b are not complete, but are terminated before 15 000 km and/or beginning beyond 3000 km, the longest and the shortest waves scanned in this study, because the solutions did not converge even after 100 days integration of the model. This is possibly due to the presence of multiple most unstable modes with nearly the same growth rates. The curves could have been completed by utilizing an eigenvalue approach to the problem, which was not attempted in this study.

The normalized meridional amplitude and phase profiles for the preferred waves in all four cases are computed from the spectral solutions and shown in Figs. 4a and 4b. The associated momentum transports are given in Fig. 5.

The divergent asymmetric case is the most general, it is expected that these results should be closest to the observations. In this case the preferred wavelength is 6500 km with an e-folding time of 6.5 days, a westward phase speed of 23.5 m s^{-1} and a period of 3.2 days as can be seen from Figs.

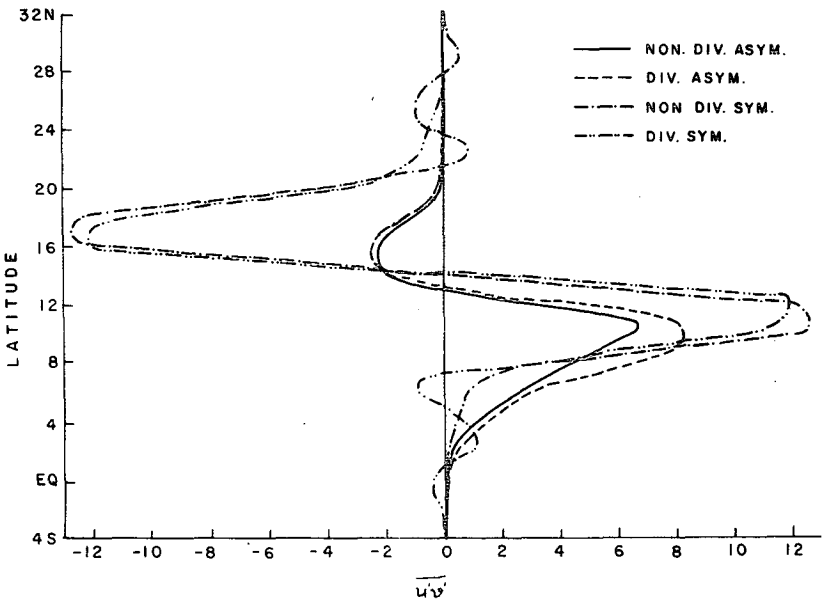

FIG. 5. Zonal momentum transport profile (in arbitrary units) by the preferred waves for the four cases.

3a and 3b. It may be added that the growth rate found for the local zonal wind profile at 80°E (not given) is much higher with an e-folding time of 2.5 days for the preferred wavelength of 6000 km. The preferred wavelengths are in close agreement with the computed wavelengths of the observed upper tropospheric waves.

Various definitions are available in the literature for the zonal scale of the waves in terms of their wavenumber k or wavelength L. The zonal wave scale defined as k^{-1} (Holton, 1972) is suitable for estimating accurately the maximum value of x-derivatives. We feel that a more appropriate criterion for a selection of the zonal scale would be that it estimates the average value of derivatives instead of their maximum value as is the case with the above definition. Based on this consideration, we propose to define $2k^{-1}$ as the zonal scale of the wave of the wavenumber k, which is also close to the half-width of the wave field distribution around its maximum. Further, $2k^{-1}$ is close to a criterion of the scale as the quarter wavelength used by Blumen (1979). The zonal scale of the preferred divergent asymmetric wave (2070 km) as obtained from the present definition is nearly equal to the Rossby radius of deformation.

Shukla (1977) has obtained a preferred nondivergent barotropic wave of 3000 km and an e-folding time of about three days for an easterly jet at the 150 mb level along the longitude 85°E, whereas the values obtained in this study for the nondivergent case are nearly twice the values obtained by Shukla. These large differences can be attributed to the very closeness of the southern boundary to the stronger easterly jet's center in his study than in the present study. Furthermore, the channel width used in the present study is considerably larger than that utilized by Shukla.

a. Effect of antisymmetric components

A comparison of asymmetric divergent and nondivergent growth rate spectra with the corresponding symmetric cases (Fig. 3a) reveals that the growth rates of the waves in the former are less than those of the latter for wavelengths less than or equal to the preferred wavelength and more for the longer waves. However, the differences in the growth rates in the long wavelength region between two divergent cases are insignificant. This perhaps is due to the predominance of the divergence effect over that of antisymmetric components on the growth rates in this region. The antisymmetric components of the jet also affected an increase in the preferred wavelengths by ~800 km. A decrease in the westward phase speed of the asymmetric waves in comparison to the symmetric waves is also seen in Fig. 3b.

The normalized meridional amplitude profiles of the preferred waves (Fig. 4a) show that the maximum amplitude of the wave is located at the jet's center (14°N) for the symmetric cases, while they are located at 6°N in the asymmetric cases. Thus, the wave amplitude maximum is shifted toward the cyclonic side by the antisymmetric components

of the jet. Furthermore, the average meridional scale of the symmetric wave is 2600 km, which is equal to the meridional scale of the basic flow, but greater than the Rossby radius of deformation. For asymmetric waves the meridional scale is 1600 km, which is less than the meridional scale of the basic flow as well as the Rossby radius of deformation, but equal to the geometric mean of the radius of curvature and the meridional scale of the basic flow. From the above discussion it may be concluded that marginally unstable barotropic waves with meridional scale less than the Rossby radius of deformation can arise for the asymmetric basic zonal flow. It may be mentioned in this connection that Stone (1969) has shown for a symmetric idealized midlatitude westerly jet that the marginally unstable baroclinic waves have a meridional scale equal to the Rossby radius of deformation [subsequently pointed out by Simmons (1974)].

Under the geostrophic approximation the square of the ratio of zonal to meridional scale of the transient wave is equal to the ratio of the zonal to meridional wind variances associated with transient eddies $\overline{\langle u'^2 \rangle}/\overline{\langle v'^2 \rangle}$, where angle brackets and an overbar represent time and zonal averages, respectively. The average ratio of the variances in the 500–100 mb layer and the latitudinal belt 10°S–30°N is computed for the season (June–August), from the values of Oort and Rasmusson (1971) and found to be 1.56. This value is very close to the square of the ratio of zonal to meridional scale of the divergent asymmetric wave in our study.

The southward shift of the asymmetric wave-amplitude maximum is connected to the presence of a large positive maximum at 4°N in $-\bar{u}_{yy}$ profile for the asymmetric jet. This feature is absent in the profile for the symmetric jet. These can easily be concluded from Fig. 2. The correlation between the locations of the wave-amplitude maximum and the large positive maximum of $-\bar{u}_{yy}$ was established by computing the solution for a modified asymmetric jet, obtained by changing the sign of the odd coefficients of the observed asymmetric jet. For the modified asymmetric jet a large positive maximum of $-\bar{u}_{yy}$ was found at 24°N and close to this latitude the preferred wave also has a maximum amplitude.

The zonal mean momentum transport profiles, $\overline{u'v'}$, associated with the normalized preferred waves of the four different cases are computed and they subsequently normalized with respect to the largest maximum transport among them. These normalized profiles are presented in Fig. 5. The transports associated with the symmetric jet are antisymmetric about its center with no transport across it, whereas the easterly momentum transports associated with the asymmetric jet are more equatorward than poleward. The poleward transports in the asymmetric case are confined in a relatively smaller latitudinal belt than the equatorward transports with the maximum value located at 10°N. A similar result regarding the momentum transports for an asymmetric westerly jet has been obtained by Mudrick (1979). The observed equatorward easterly momentum transport, in the 70–120°E belt, has a maximum at the equator (Newell *et al.*, 1972). This observed maximum may be due to the large contributions of the equatorial waves, which are not considered in this study.

The computed barotropic energy conversions indicate that the waves are receiving kinetic energy from the basic wind. The conversions in the asymmetric cases are nearly one-half of the conversions in symmetric cases, in spite of the fact that the preferred waves in the two cases have comparable growth rates. In this connection it may be pointed out that the wave amplitudes are essentially confined to a narrower belt in the former compared to the latter. This indicates that the normalized waves in the former have much less kinetic energy and, consequently, require the less energy conversions than the latter for the similar growth rates. This explains why the energy conversions are not inconsistent with the growth rates in the two cases.

b. Effect of divergence

A comparison between growth rate spectrum of divergent cases with the respective nondivergent cases (Fig. 3a) shows that the divergence has a destabilizing effect at all the wavelengths. However, this effect is more pronounced for the waves longer than the preferred wave. Furthermore, the preferred waves are found to shift by (about) 1000 km toward the longer wavelengths in the divergent cases compared to nondivergent cases. A similar increase in the growth rates of longer waves and an increase in the preferred wavelength due to the effect of divergence can be seen in the results of Kuo (1978) obtained by using a primitive equation model. The above destabilization of the waves in an easterly jet due to the divergence effect is related to the reduction in the effective value of beta. The effect of divergence on the meridional distribution of the amplitude and the phase tilt of the wave is insignificant, except for the unusually large tilt on the north side of the jet that is found for the nondivergent asymmetric wave (Fig. 4b). The divergence increases the magnitude of the maximum equatorward easterly momentum transport relative to the poleward transport for the asymmetric wave. It seems that the divergence effect also contributes toward bringing the model wave closer to the characteristics associated with the observed disturbances in respect of the momentum transports.

6. Conclusions

The antisymmetric part in the easterly jet causes a decrease (increase) of growth rates in the short wavelengths (long wavelength) region and also a considerable southward shift in the location of the preferred wave-amplitude maximum. The asymmetric wave-amplitude maximum is located near the large positive maximum of $-\bar{u}_{yy}$. Due to this shift of amplitude maximum, the northward transport of zonal momentum is greatly diminished without much decrease in southward transport. Another important contribution of the antisymmetric part is in the considerable reduction in the meridional scale of the preferred wave. It has been shown that the meridional scales of the preferred waves are more closely related to the meridional scale of the basic flow than to the Rossby radius of deformation. Furthermore, it has been found that the zonal scale of the asymmetric divergent preferred wave is nearly equal to the Rossby radius of deformation.

It has been found that the maximum growth rate is increased and is shifted toward a longer wavelength by the divergence. The zonal and meridional scales of the divergent asymmetric wave as obtained in this study are in close agreement with the computed values for the observed upper tropospheric waves in the tropics. Even though the computed growth rates appear to be small, their effectiveness in exciting the waves in the vicinity of the easterly jet, where the dissipation rates are small, should not be underestimated. Also, the local growth rates at certain longitudes (80°E) are much higher than the values obtained from the averaged jet, thereby making the barotropic instability mechanism a significant physical process for generating the upper level disturbances. It may be emphasized that the results obtained in this study do not rule out the possible contributions from the other forms of instabilities, in particular the baroclinic instability to the generation and the growth of the upper level waves.

Though we have discussed earlier the validity of quasi-geostrophic approximation in the tropical belt as a whole, the occurrence of asymmetric wave-amplitude maximum close to the equator has necessitated closer examination of this approximation near the equator. In this connection it may be noted that Krishnamurti (1971) has shown that even close to the equator the irrotational component of the wind is smaller than the rotational component of the wind for all synoptic scales of the 200 mb summer flow.

Acknowledgments. The authors are thankful to Dr. Bh.V. Ramana Murty, Director, Indian Institute of Tropical Meteorology, Pune, for continuous encouragement. The authors appreciate the anonymous reviewers' suggestions which led to a significant improvement in the presentation of the paper. We also thank Mrs. V. V. Savant for typing the manuscript. Utilization of the computing facility at the India Meteorological Department, Pune, also is acknowledged.

REFERENCES

Blumen, W., 1979: Unstable nonlinear evaluation of an Eady wave in time-dependent basic flows and frontogensis. *J. Atmos. Sci.*, **36**, 3–11.

Colton, D. E., 1973: Barotropic scale interactions in the tropical upper troposphere during the northern summer. *J. Atmos. Sci.*, **30**, 1287–1302.

Haltiner, G. J., and R. T. Song, 1962: Dynamic instability in barotropic flow. *Tellus*, **4**, 383–393.

Holton, J. R., 1972: *An Introduction to Dynamic Meteorology*. Academic Press, 319 pp.

Kanamitsu, M., T. N. Krishnamurti and C. G. Depardine, 1972: On scale interactions in the tropics during northern summer. *J. Atmos. Sci.*, **29**, 698–706.

Koteswaram, P., 1958: The easterly jet stream in the tropics. *Tellus*, **10**, 43–57.

Krishnamurti, T. N., 1971: Observation study of the tropical upper tropospheric motion field during the Northern Hemisphere summer. *J. Appl. Meteor.*, **10**, 1066–1096.

Kuo, H. L., 1978: A two-layer study of the combined barotropic and baroclinic instability in the tropics. *J. Atmos. Sci.*, **35**, 1840–1860.

Lipps, F. B., 1963: Stability of jets in a divergent barotropic fluid. *J. Atmos. Sci.*, **20**, 120–129.

——, 1966: Momentum transfer across an asymmetric jet. *J. Atmos. Sci.*, **23**, 213–222.

Mishra, S. K., and P. S. Salvekar, 1980: Role of baroclinic instability in the development of monsoon disturbances. *J. Atmos. Sci.*, **37**, 383–394.

Mudrick, E. D., 1979: On the instability of asymmetric jets. *J. Atmos. Sci.*, **36**, 1217–1225.

Newell, R. E., J. W. Kidson, D. G. Vincent and G. J. Boer, 1972: *The General Circulation of the Tropical Atmosphere and Interactions with Extratropical Latitudes*, Vol. 1. MIT Press, 258 pp.

Oort, A. H., and E. R. Rasmusson, 1971: *Atmospheric Circulation Statistics*. NOAA Prof. Pap. 5, U.S. Govt. Printing Office, Washington, DC, 323 pp.

Philander, S. G. H., 1976: A note on the stability of tropical easterlies. *J. Meteor. Soc. Japan*, **54**, 328–330.

Robert, A. J., 1966: The integration of low order spectral form of the primitive meteorological equations. *J. Meteor. Soc. Japan*, **44**, 237–245.

Shukla, J., 1977: Barotropic-baroclinic instability of mean zonal wind during summer monsoon. *Pure Appl. Geophys.*, **115**, 1449–1461.

Simmons, A. J., 1974: The meridional scale of baroclinic waves. *J. Atmos. Sci.*, **31**, 1515–1525.

Stone, P. H., 1969: The meridional structure of baroclinic waves. *J. Atmos. Sci.*, **26**, 376–389.

Tupaz, J. B., R. T. Williams and C. P. Chang, 1978: A numerical study of barotropic instability in a zonally varying easterly jet. *J. Atmos. Sci.*, **35**, 1265–1280.

Wiin-Nielson, A., 1961: On short- and long-term variations in quasi-geostrophic flow. *Mon. Wea. Rev.*, **89**, 461–476.

Yamasaki, M., and M. Wada, 1972: Barotropic instability of an easterly zonal current. *J. Meteor. Soc. Japan*, **50**, 110–121.